

Investigation of the interactions between silver nanoparticles and HeLa cells by scanning electrochemical microscopy†‡

Zhong Chen,^a Shubao Xie,^a Li Shen,^a Yu Du,^a Shali He,^a Qing Li,^a Zhongwei Liang,^a Xin Meng,^a Bo Li,^a Xiaodong Xu,^a Hongwei Ma,^b Yanyi Huang^b and Yuanhua Shao^{*a}

Received 25th April 2008, Accepted 18th July 2008

First published as an Advance Article on the web 29th July 2008

DOI: 10.1039/b807057a

The interactions between HeLa cells and silver nanoparticles (AgNPs) have been studied by scanning electrochemical microscopy (SECM) with both $\text{IrCl}_6^{2-/3-}$ and $\text{Fe}(\text{CN})_6^{3-/4-}$ as the dual mediators. IrCl_6^{2-} , which can be produced *in situ* and react with AgNPs, is used as the mediator between the AgNPs on the cells and the SECM tip. Another redox couple, $\text{Fe}(\text{CN})_6^{3-/4-}$, which has a similar hydrophilicity to $\text{IrCl}_6^{2-/3-}$, but cannot react with AgNPs, is also employed for the contrast experiments. The cell array is cultured successfully onto a Petri dish by microcontact printing (μCP) technique, which can provide a basic platform for studying of single cells. The approach curve and line scan are the two methods of SECM employed here to study the HeLa cells. The former can provide the information about the interaction between HeLa cells and AgNPs whereas the later gives the cell imaging. The permeability of cell membranes and morphology are two main factors which have effects on the feedback mode signals when $\text{K}_3\text{Fe}(\text{CN})_6$ is used as the mediator. The permeability of the cell membranes can be ignored after interaction with high concentration of AgNP solution and the height of the HeLa cells is slightly decreased in this process. The kinetic rate constants (k^0) between IrCl_6^{2-} and Ag on the HeLa cell can be evaluated using K_3IrCl_6 as the mediator, and they are increased with the higher concentrations of the AgNP solutions. The k^0 is changed about 10 times from $0.43 \pm 0.04 \times 10^{-4}$ to $1.25 \pm 0.07 \times 10^{-4}$ and to $3.93 \pm 1.9 \times 10^{-4} \text{ cm s}^{-1}$ corresponding to 0, 1 and 5 mM of AgNO_3 solution. The experimental results demonstrate that the AgNPs can be adsorbed on the cell surface and detected by SECM. Thus, the amount of AgNPs adsorbed on cell membranes and the permeability or morphology changes can be investigated simultaneously using this approach. The dual mediator system and cell array fabricated by μCP technique can provide better reproducibility because they can simplify experiments, and provide a platform for further single cell detection.

Introduction

Scanning electrochemical microscopy (SECM), an *in situ* technique, which has allowed one to study different types of interfaces and surfaces electrochemically with high spatial and temporal resolution, has previously been used to investigate biological systems.¹⁻⁴ In the initial SECM investigations of biological samples by Bard *et al.* in 1990, the topographic images of surfaces of grass and *Ligustrum sinensis* leaves were obtained and the photosynthesis process was evaluated by the reduction of oxygen produced from an *Elodea* leaf.⁵

After that, the SECM has been increasingly employed for studying the living biological systems, and attempts have been recently undertaken in several aspects. For example, Matsue and coworkers have studied the metabolism, respiration and photosynthesis activities of a variety of individual living cells using generation-collection mode.⁶⁻¹² Mirkin *et al.* have measured the intracellular redox activity and topography of different mammalian cell lines with hydrophobic mediators, which can diffuse across the cell membrane and react with the redox center in the cell using feedback mode of SECM.^{13,14} Schuhmann *et al.* have detected nitric oxide (NO) released from growing endothelial cell monolayers upon stimulation with a chemically modified NO-sensing microelectrode as the tip of SECM.¹⁵⁻¹⁷ Recently, Bard and coworkers have monitored and detected the export of thiodione, which was produced by the conjugation of glutathione and cytotoxic menadione in the living cells.^{18,19} They also reported that a liquid/liquid interface-based micropipette sensor could be used to monitor the toxicity of Ag^+ to fibroblast cells.²⁰ Jin's group has developed an electrochemical method for determination of enzyme activity inside single cells quantitatively by using a nanolitre-scale microcell.^{21,22} The combination of SECM and microbial array chips was also applied for

^aBeijing National Laboratory for Molecular Sciences, Institute of Analytical Chemistry, College of Chemistry and Molecular Engineering, Peking University, Beijing, 100871, China

^bCollege of Engineering, Peking University, Beijing, 100871, China.
E-mail: yhshao@pku.edu.cn; Fax: +86-10-62751708;
Tel: +86-10-62759394

† This paper is part of an *Analyst* themed issue highlighting Chinese science, with guest editor Mengsu (Michael) Yang.

‡ Electronic supplementary information (ESI) available: Fig. S1, experiment for the lateral scanning over the silver nanoparticles spots with different mediators. See DOI: 10.1039/b807057a

detecting recombinant proteins²³ and metabolic alteration in bacteria.²⁴ Besides those studies, the permeability of the cell membranes to several types of redox couples was monitored by the feedback mode of SECM. Negative feedback signals were usually obtained with hydrophilic mediators (e.g., ferrocyanide or ferrocenecarboxylate), which could not pass through the cell membrane. In contrast, hydrophobic mediators (e.g., quinones such as menadione and 1,2-naphthoquinone) could diffuse across the cell membrane and react with redox moieties inside the cell, resulting in positive feedback signals.²⁵ The tip current can be used to determine the effective kinetic rate constant of the overall process. Local permeability of the nuclear envelope at large intact nuclei isolated from *Xenopus laevis* oocytes was also studied by SECM.²⁶ All those studies demonstrate that SECM is a promising technique for the investigation of living single cells.

It is usually difficult to study cells or bacteria quantitatively at the single-cell level by SECM when the diameter of the SECM tip is comparable with the size of an individual cell.²⁰ To make further progress in the development of the SECM based cellular sensing systems, it will be undoubtedly required to place cells in predetermined locations with defined shapes and sizes.²⁷ In this way, it is easier to eliminate the effect of other cells around or near the cell under studied, and obtain more reliable information. Another approach is to employ a much smaller size of SECM tip, for instance, Mirkin *et al.* reported recently the electrochemical behavior of mammalian cells by SECM with nanoelectrodes as the tip.²⁸ Microfabrication combined with surface chemistry and material science has provided a new possibility for further investigating the interactions of anchorage-dependent cells with their environments.²⁹ A versatile ensemble of methods was developed during the last decade. For example, micro-contact printing (μ CP), a soft lithography technique, is commonly used to create chemical structures on surfaces for controlling cell-substrate interactions. This method uses an elastic stamp with micrometre-scale features, which made from poly(dimethylsiloxane) (PDMS), for making monolayer patterns of blocking effect to the adsorption of extracellular matrix (ECM) proteins. Chilkoti and coworkers have reported a simple and generic method to micro-patterning surfaces with an amphiphilic comb polymer presenting short oligoethylene glycol side chains, which can prevent the non-specific adsorption of ECM proteins during cell culture.³⁰ Single cell arrays can be easily obtained using such an approach through variation of the size of pattern.

The understanding of interactions between metal nanoparticles and living systems is of fundamental and practical interest due to metal particles in the nanometre size range that exhibit unique physical and chemical properties, different from both the ion and the bulk material themselves. Although the silver ion has long been known to have strong toxicity to a wide range of micro-organisms,³¹ the cytotoxicity of AgNPs has only been studied recently owing to the demands of the application of nanotechnology to biosystems. The practical application of the analysis of nucleolar organizer regions (NORs) in tumor pathology began in 1986, when a simple argyrophilic technique (silver-stained nucleolar organizer regions, AgNOR) to detect proteins associated with NORs was described.³² At present, the evaluation of AgNOR quantity can be regarded as an indicator of prognosis.³³

The interactions between the AgNPs and the bacteria or cancer cells could be partially identified in three ways:^{33–35} (1) attaching to the surface of the cell membrane and disturbing its proper function, like permeability; (2) penetrating into the cell and causing further damage by possibly interacting with sulfur- and phosphorus-containing compounds such as DNA or NORs; (3) releasing silver ions, which will have an additional contribution to the bactericidal effect of the AgNPs. In previous work, scanning electron microscopy (SEM) was a common tool, which can be employed to investigate the change of cell morphologies under the attachment of AgNPs on the surface.³⁶ However, it is hard to obtain the further information like the permeability of the cell membranes by this way. Girault's group has shown that the silver stained proteins adsorbed on poly(vinylidene difluoride) (PVDF) membranes can be imaged by SECM and developed a readout tool for detection of proteins with high sensitivity.^{37,38} This method actually provides a basis for the current studying of the interaction between cells and AgNPs by SECM.

In this work, we have tried to study the interaction between AgNPs and HeLa cells by SECM with both $\text{K}_3\text{Fe}(\text{CN})_6$ and K_3IrCl_6 as mediators in the same solution. A cell-resistant polymer, an amphiphilic comb polymer, was patterned onto a Petri dish using the μ CP method, and then the HeLa cell array could be obtained when culturing the HeLa cells in proper experimental conditions. $\text{IrCl}_6^{2-/3-}$, which can react with AgNPs, serves as the mediator to study the effect of the amount of AgNPs adsorbed on the cell membranes on the kinetic rate constants, whereas $\text{Fe}(\text{CN})_6^{3-/4-}$, which cannot react with AgNPs, has been used as the mediator to study the varying of the permeability or morphology of cell membranes when adding AgNP solution to the cell array. We have demonstrated that both mediators can be used simultaneously and have no interaction with each other during the detection. This will benefit the investigation because one does not need to change the solution in the process, which will make the results more compatible and reproducible.

Experimental

Chemicals and materials

All chemicals were used as received. Potassium hexachloro-iridate(III) (K_3IrCl_6 , Aldrich); potassium ferricyanide(III) ($\text{K}_3\text{Fe}(\text{CN})_6$), sodium nitrate (NaNO_3 , >99%), silver nitrate (AgNO_3 , >99.5%), methanol and sodium borohydride (all supplied by Beijing Chemicals Co., Beijing, China). PVDF membranes (0.2 μm , Millipore). All aqueous solutions were prepared from the Millipore water (Milli-Q, Millipore Corp.).

Comb polymers were synthesized according to the previously reported procedures, consisting of methyl methacrylate (MMA), poly(ethylene glycol methyl ether methacrylate) (referred herein as hydroxyl-poly(oxyethylene methacrylate) (HPOEM)), and poly(oxyethylene methacrylate) (POEM) *via* free-radical polymerization with a range of compositions.³⁹

Synthesis of AgNPs

AgNPs were prepared by reduction of AgNO_3 using NaBH_4 . In a 250 mL three-neck flask, 100 mL of AgNO_3 (the concentration was 1 mM or 5 mM) was stirred with the addition of a

little excess amount of NaBH_4 . Within very short time, the color changed from colorless to brown or black (the color of the nanoparticles solution changed with the concentrations of AgNO_3). The prepared nanoparticles were characterized with transmission electron microscopy (TEM) (JEM 200CX, JEOL), and the size was determined to be 30–50 nm. They are easily to be coagulated without adding protected compound which will decrease the activity of the nanoparticles, therefore the AgNPs were freshly prepared before used. It is not easily to determine the concentration of AgNP solution so we use the concentration of AgNO_3 solution (low: 1 mM; high: 5 mM) instead.

Preparation of silver clusters on the PVDF membrane

The PVDF is hydrophobic, and it is necessary to be first wetted in methanol for 1–3 s and then immersed in water for 1–2 min to elute the methanol.^{37,38} Once the membrane has been wetted with water, do not allow it to be dry until the AgNPs adsorbed on it. The AgNP solution was spotted on the membranes by a microsyringe, and the diameters of the spots were about 1 mm. After evaporation of the solution, the AgNPs spot was slight black and the membrane can be characterized by SECM. The mediators were 1 mM $\text{K}_3\text{Fe}(\text{CN})_6$ and 1 mM K_3IrCl_6 with 150 mM NaNO_3 as the supporting electrolyte, and its concentration is similar to the commonly used physiological saline solution. This complex solution was also be used to study HeLa cells in the following step.

Cell culture and SECM measurements

The cell array was prepared after comb polymer was micropatterned using an oxidized poly(dimethylsiloxane) (PDMS) stamp which can provide micrometre-sized negative features based on the method reported previously.³⁰ Briefly, the PDMS molds were fabricated by casting a polymer precursor (Sylgard 184 from Dow Corning) against a photoresist master that was fabricated by photolithography, then the viscous base and the curing agent (10 : 1 ratio by weight) were mixed well and cured at 80 °C for 2 h. The resulting PDMS stamp was 0.5 cm thick and cut into 1 cm × 1 cm pieces for further application. The stamp was immersed in a 1% (w/v) solution of the comb polymer in a 50 : 50 (v/v) H_2O /ethanol mixture and brought into conformal contact with the bottom of the culture dish, resulting in the transfer of the comb polymer to the regions of the surface that were in contact with the stamp.

The HeLa cells were grown in Dulbecco's Modified Eagle's Medium (DMEM) supplemented with 10% fetal bovine serum (FBS), 100 units mL^{-1} penicillin, 100 $\mu\text{g mL}^{-1}$ streptomycin, at 37 °C in 5% CO_2 . The cells were incubated for 24 h, and after that we could obtain the cell array because the micropatterned comb polymer is cell-resistant.

A Nikon TE-2000 inverted microscope (Nikon Co., Japan) was used to observe the coverage and growth status of the HeLa cells. SECM and cyclic voltammetric (CV) measurements were performed with a CHI 910B workstation (CH Instrument Co., Austin, TX) which mounted on the stage of the inverted microscope. The three-electrode system consisted of a 12.5 μm radius Pt working electrode, an Ag/AgCl electrode as the reference electrode, and a Pt wire as the auxiliary electrode.

Before the measurement, the physiological saline solution was replaced by 150 mM NaNO_3 , and then added the newly synthesized AgNP solution. The interaction of AgNPs and cells was limited to 10 min, and then the cells were washed using 150 mM NaNO_3 solution twice carefully to repulse the excessive silver nanoparticles in the solution, and detected by SECM in 150 mM NaNO_3 solution with 1 mM K_3IrCl_6 and 1 mM $\text{K}_3\text{Fe}(\text{CN})_6$ as the mediators.

Results and discussion

Characterization of silver clusters on the PVDF membrane by SECM

In order to test the dual-mediator system, we have chosen the well studied PVDF membrane as a model system for living cells. Based on the previous work,^{37,38,40} we know that there are two possible mechanisms for the signal generation between the SECM tip and AgNPs. One is the conventional feedback mode which depends upon the inherent sensitivity of SECM to the detection of small variation of the surface conductivities, as described in ref. 40. In this case, it requires a large amount of interconnected silver clusters to provide a conductive substrate. The other is an etching process of AgNPs induced by the SECM tip, which relies on a bimolecular electron transfer (ET) reaction between an oxidation species formed at the tip and AgNPs deposited on a substrate (PVDF membrane or a living cell). In the dual-mediator system, $\text{K}_3\text{Fe}(\text{CN})_6$ and K_3IrCl_6 , based on these two mechanisms, respectively, are chosen as the mediators to detect the silver clusters deposited on PVDF membranes, which can be used as the model for study of the interaction between cells and AgNPs. The cyclic voltammograms shown in Fig. 1 are observed on a 25 μm diameter Pt electrode with (solid curve) or without the redox couples (dash line). The two redox couples are having almost the same steady-state current because they have the same concentrations (1 mM for each other), similar diffusion coefficients ($7.6 \times 10^{-6} \text{ cm}^2 \text{ s}^{-1}$ for $\text{K}_3\text{Fe}(\text{CN})_6$ and $8.2 \times 10^{-6} \text{ cm}^2 \text{ s}^{-1}$ for K_3IrCl_6)⁴¹ and the same charge involved

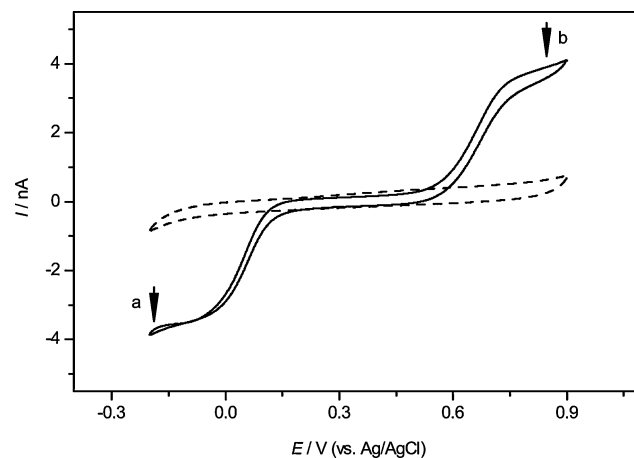
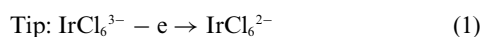


Fig. 1 The cyclic voltammograms obtained by the Pt microelectrode in the 150 mM NaNO_3 solution as the blank (dash line) or including 1 mM K_3IrCl_6 (b) and 1 mM $\text{K}_3\text{Fe}(\text{CN})_6$ (a) (solid line) as the mediators. The scan rate was 10 mV s^{-1} , and Ag/AgCl served as the reference electrode. The arrows indicate the tip voltage for each mediator during the SECM experiments.

in the redox processes in the system with 150 mM NaNO₃ as the supporting electrolyte. These CV curves indicate that the half-wave potentials on the tip are about 0.05 V for K₃Fe(CN)₆, and 0.65 V for K₃IrCl₆ (vs. Ag/AgCl). More importantly, they do not interfere each other.

Using the same solution containing K₃Fe(CN)₆ and K₃IrCl₆, two series of data for SECM lateral scans over the same position with each of them as mediator have been obtained (see ESI†). The signals based on K₃IrCl₆ are about five times larger than those based on K₃Fe(CN)₆. This is because the Fe(CN)₆⁴⁻ (generated by the tip reaction) cannot react with the AgNPs, which only act as an insulating substrate, while IrCl₆²⁻, which has a more positive standard potential, can oxidize the AgNPs into Ag⁺ and cause the enhancement of the SECM feedback signals:



Girault *et al.* have demonstrated that SECM can be employed as a sensitive and quantitative readout method for the detection of proteins adsorbed on PDVF membranes after stained by AgNPs, based on similar reactions.³⁷

Approach curve above a single living Hela cell

The combination of microfabrication and scanning probe techniques is useful for studies of single cells. From the diagram shown in Fig. 2A obtained by optical microscopy, it is clearly that the cell array was cultured successfully onto a Petri dish. The pattern can be varied according to our purpose. In the present experiments, the size of the “cell island” is about 20 μm in diameter, and the distance between two nearest “cell islands” is about 30 μm. Almost all the cells will be separated each other, but there are still some cells striding over two “islands”, which

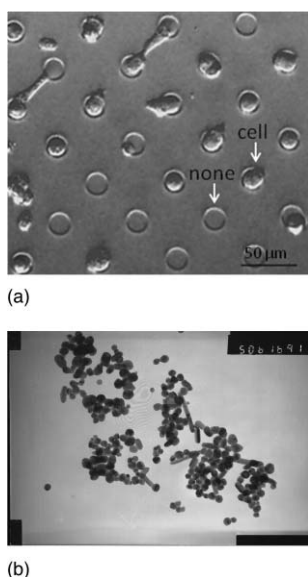


Fig. 2 (a) The cell array cultured onto the Petri dish, pictured by the inverted microscopy. The diameter of cell island is about 20 μm and the distance between two nearest islands is about 30 μm. (b) The TEM image of AgNPs, and the diameters of them were between 30–50 nm.

will be very interesting to be studied in the future. There are also some blank islands without cells, which is rather common when the cells' density is not high enough. In order to investigate the interaction between AgNPs and Hela cell, the newly prepared AgNPs should be pre-mixed with the cell array, and then incubated at room temperature for 10 min. Fig. 2B is the TEM diagram of the freshly prepared AgNPs with a diameter about 30–50 nm.

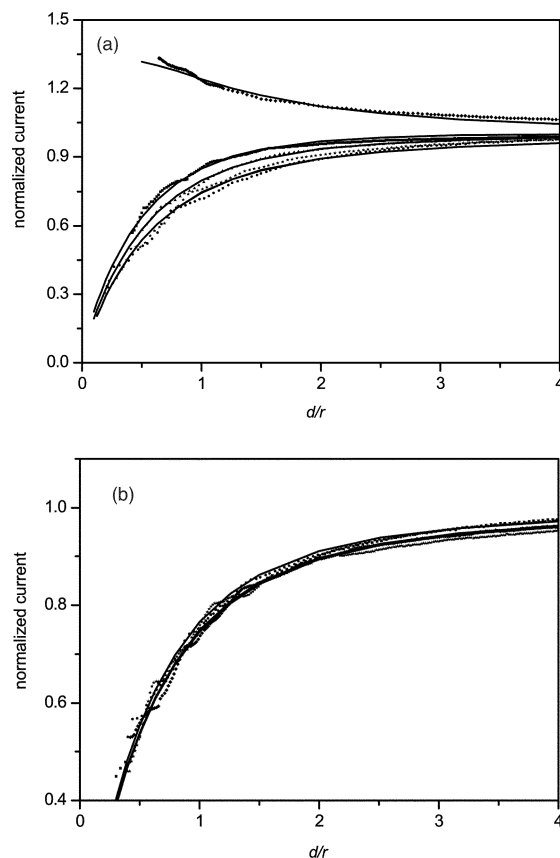


Fig. 3 Normalized approach curves. Five curves are shown in (A) using K₃IrCl₆ as the redox mediator, from top to the bottom are: (1) PVDF + AgNPs, (2) Hela cell + AgNPs (high concentration), (3) Hela cell + AgNPs (low concentration), (4) Hela cell, (5) PVDF. Four curves are shown in (B) using K₃Fe(CN)₆ as the redox mediator, from top to the bottom are (1) PVDF + AgNPs, (2) Hela cell + AgNPs (large concentration), (3) Hela cell, (4) PVDF. The tip potential was held at 0.65 V for K₃IrCl₆ and 0.05 V for K₃Fe(CN)₆ (vs. Ag/AgCl). The approach rates are 10 μm s⁻¹.

After finding a Hela cell and positioning the SECM tip above it, with the help of the optical microscope, the current–distance (approach) curves can be obtained, which are shown in Fig. 3, and the relevant kinetic rate constants can be obtained by fitting the experimental curves to the theoretical ones (see Table 1). Fig. 3A shows the approach curve for the case when K₃IrCl₆ is used as the mediator. Positive feedback is observed when approaching the AgNP clusters adsorbed on PVDF membrane, which is consistent with the line scan results in the previous section (see ESI†). The effective heterogeneous kinetic rate constants (*k*⁰) of reactions between K₃IrCl₆ and different substrates are evaluated and listed in Table 1. The rate constant for the cell without AgNPs is similar to that of the PVDF as the substrate,

Table 1 The kinetic rate constants of the Hela cells or PVDF before and after the interactions with AgNPs using different mediators (repeated 4 times for each case)

Substrate	Rate constant (k^0) $\times 10^{-4}/\text{cm s}^{-1}$	
	Mediator (1 mM)	
	K_3IrCl_6	$\text{K}_3\text{Fe}(\text{CN})_6$
PVDF	0.45 ± 0.07	0.45 ± 0.05
PVDF + AgNPs	50.0 ± 3.0	0.85 ± 0.07
Cell	0.43 ± 0.04	0.45 ± 0.07
Cell + AgNPs (low concentration)	1.25 ± 0.07	—
Cell + AgNPs (high concentration)	3.93 ± 1.9	0.55 ± 0.06

and negative feedback is obtained. Fig. 3B shows the case when $\text{K}_3\text{Fe}(\text{CN})_6$ is used as the mediator. All the feedback curves are almost overlapping each other, which indicates that the reaction between the mediator and cell or AgNPs is very slow.

According to our results and previous reports, there are at least three factors influencing the feedback signals in SECM experiments using $\text{Fe}(\text{CN})_6^{4-}$ and IrCl_6^{2-} as redox mediators for the same cell array: (1) the reaction between the mediators and AgNPs adsorbed on the cell membrane, (2) the permeability of the cell membrane for the mediators, (3) the reaction between the mediators and intracellular redox species (see Fig. 4). The permeability is depended mainly on the hydrophilicity of mediator and the perforation in cell membrane after interaction with AgNPs. Since the hydrophilicity is similar for $\text{Fe}(\text{CN})_6^{4-}$ and IrCl_6^{2-} , and the interaction process between cell and AgNPs is identical in our experiments, so the permeability for the two mediators should be similar. From Fig. 3B and Table 1, the rate constants for the Hela cell before and after the interaction with AgNPs have no significant difference when $\text{K}_3\text{Fe}(\text{CN})_6$ is used as the mediator. Therefore, the change of permeability of the cell membrane can be ignored in this process and there is no perforation in these concentrations of AgNPs. It has

been reported that after treatment with AgNPs, perforation appears in the bacteria cell membranes,³⁶ which will change the cell permeability, but the constitution and configuration of the membranes in bacteria and cancer cells are quite different from each other, so that the perforation may not appear in the current studies. That is, such hydrophilic mediators will still hardly be able to pass through the cell membrane and react with the intracellular redox species. Hence the signal differences between the two mediators are mainly attributed to the interactions between the SECM tip and AgNPs deposited on the Hela cells or species on the cells' surfaces, and processes 2 and 3 shown in Fig. 4 can be ignored in the present work. After interaction with AgNPs, the Hela cell shows a larger rate constant using K_3IrCl_6 as mediator, but still smaller than AgNPs clusters adsorbed on PVDF as the substrate. This is probably because the density of AgNPs adsorbed on the cell membrane is smaller than that adsorbed on the PVDF. The cell after interaction with a higher concentration of AgNP solution shows a higher rate constant than the one with a smaller concentration, which means the amount of AgNP adsorbed on the cell membranes is increased with the higher concentration of AgNP solution. These experimental results demonstrate that we can investigate simultaneously the permeability of cell membranes using $\text{K}_3\text{Fe}(\text{CN})_6$ as the mediator and the effect of the amount of AgNPs adsorbed on the Hela cell membranes using K_3IrCl_6 as the mediator.

Imaging the cell array

An approach curve was taken to control the distance between the tip and the bottom of the Petri dish over a region without cells. The tip is stopped when the current is 30% of the steady-state current, which is about $3 \mu\text{m}$ from the Petri dish according to the theoretical calculation.¹⁻³ Then the SECM tip is withdrawn $15 \mu\text{m}$ to avoid touching of the cells. Thus, the tip is moved to the cell array to perform the probe scanning laterally experiments with the help of the inverted microscopy. The interaction process between Hela cells and AgNPs is similar to that previously described. The negative feedback currents of the two mediators are almost the same (see Fig. 5A) in the absence of AgNPs, indicating the cells only act as obstacles when there are no AgNPs on the cell membranes, and there is no communication between the cells and the SECM tip, or it is too small to be detected by this method. While in Fig. 5B, the negative feedback currents of K_3IrCl_6 are obviously smaller than those of $\text{K}_3\text{Fe}(\text{CN})_6$ in the presence of AgNPs, which is partially because of the adsorption of the AgNPs on the cell membranes. The negative feedback signals of K_3IrCl_6 are decreased with the increasing of AgNP concentrations and the positive feedback signals are observed ultimately (Fig. 5C). These results demonstrate that the amount of the AgNPs deposited on the cell membranes depends on the AgNP concentration in the solution, which is consistent with the results obtained in the previous section. According to the Brønsted acid–base theory, silver will tend to have a higher affinity to react with phosphorus and sulfur compounds, which are plentiful in cell membrane proteins,³⁵ therefore the AgNPs can be deposited on the Hela cell membranes randomly.

Although $\text{Fe}(\text{CN})_6^{4-}$ cannot oxidize the silver as we have demonstrated in the previous sections, the negative feedback

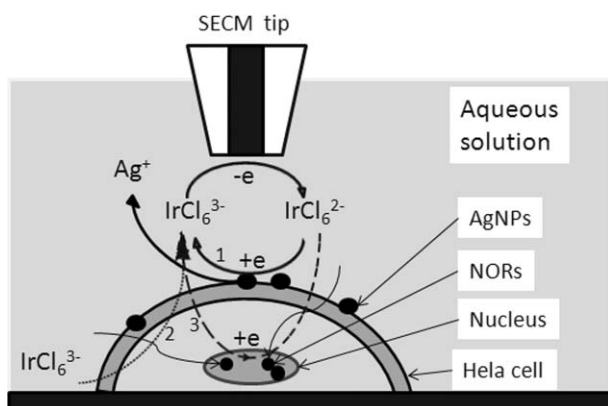


Fig. 4 The operating principle of SECM to detect the interaction between AgNPs and Hela cells. When the tip approaches the cell, the IrCl_6^{3-} is regenerated in three ways: (1) IrCl_6^{2-} reduced by the AgNPs adsorbed on the cell membranes; (2) IrCl_6^{3-} , which is plentiful in the bulk solution, may penetrate into cells and diffuse away from the tip; (3) IrCl_6^{2-} penetrates into the cells and is reduced by intracellular redox species or the AgNPs in the NORs.

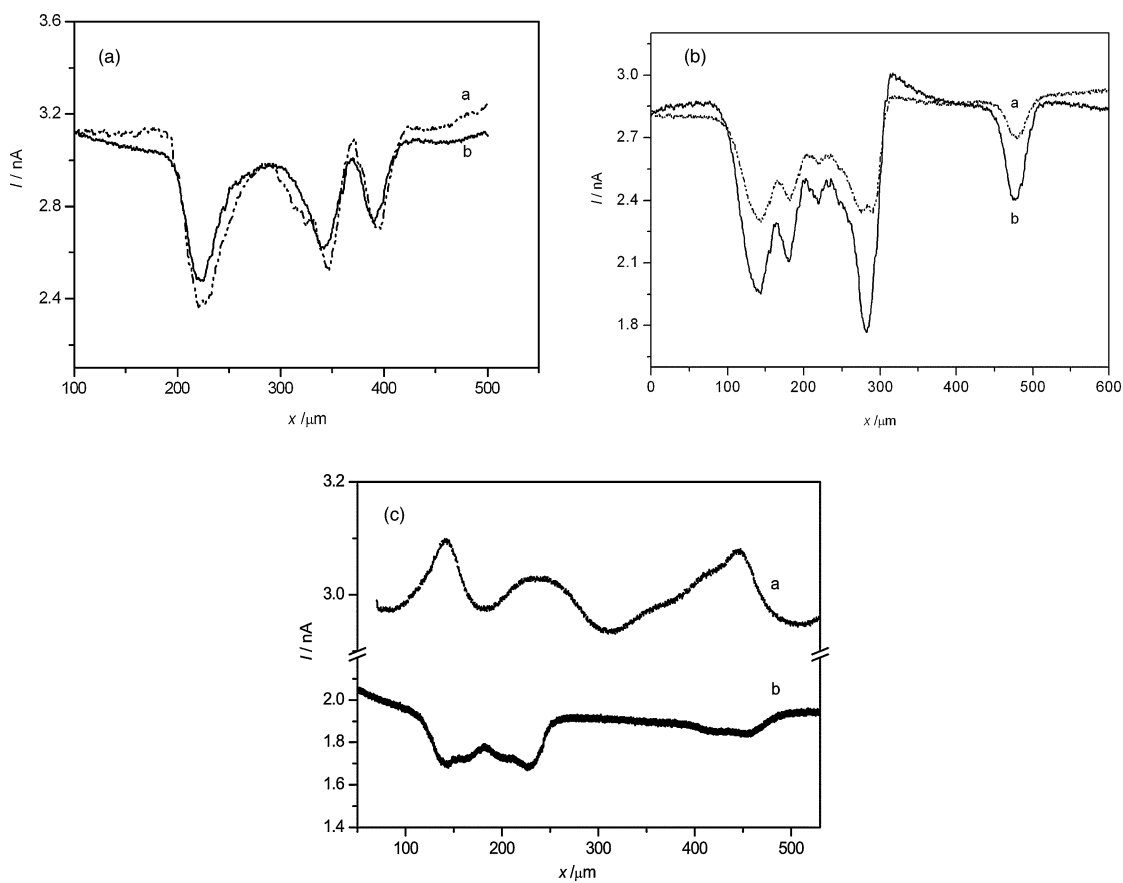


Fig. 5 Feedback currents for the lateral scanning of the HeLa cell arrays using (a) K_3IrCl_6 and (b) $\text{K}_3\text{Fe}(\text{CN})_6$ in 150 mM NaNO_3 . There were no silver nanoparticles (A) or different concentrations (B: low, C: 10 times greater than that of B) of AgNPs interacting with the HeLa cells. The scan rate was $30 \mu\text{m s}^{-1}$.

currents using $\text{K}_3\text{Fe}(\text{CN})_6$ as a mediator are a little decreased with the increasing of the concentration of AgNP (the ratios of peak current and background current are 0.78 ± 0.07 for Fig. 5B and 0.90 ± 0.04 for Fig. 5C, see Table 2). The permeability of cell membranes or the heights of the cell are two factors which will influence the feedback signals during a constant height scan above the cell arrays. A similar method was used by Baur *et al.*^{42,43} to study the morphology of PC12 cells. In the previous section, we demonstrated that the permeability has little change after interaction with AgNPs, so this difference is probably due to the height of the HeLa cells being decreased at higher concentrations of AgNPs.

SECM can also be employed for electrochemical mapping of redox activity of individual living cells. Constant height and constant distance are the two commonly used modes for the

Table 2 The ratios of peak and the background currents in the line scan curves above the cell arrays. The experimental conditions are same as in Fig. 5 (repeat 5 times for each case)

Current ratio	Mediators (1 mM)	
	K_3IrCl_6	$\text{K}_3\text{Fe}(\text{CN})_6$
A	0.81 ± 0.06	0.85 ± 0.05
B	0.87 ± 0.06	0.78 ± 0.07
C	1.0 ± 0.02	0.90 ± 0.04

SECM imaging. Schuhmann and coworkers have introduced a shear-force based constant-distance approach to control the SECM tip precisely,^{44,45} but the constant height mode is technically simple and easy to be used. Fig. 6A and C show images of the cell array obtained by the SECM constant height mode. The redox activity maps obtained by SECM are compared with the optical micrographs captured for the same fields (Fig. 6B and D). Pure negative feedback imaging of the HeLa cell array without adding AgNPs can be obtained in the presence of K_3IrCl_6 . On the contrary, positive feedback imaging can be also obtained after the interaction with higher concentration of AgNPs and cells. These phenomena are consistent with the lateral scan of the cell array. We noticed that the sizes of cells imaged by SECM were slightly larger than those obtained by the optical method. This is probably because the electrochemical signals of the mediators detected by the tip were in a diffusion field, so that the results were larger than the real size. After the interaction with AgNPs with high density, the activity of cells decreased and some of them were easy to glide from “cell islands” indicating by the red circles in Fig. 6C. This may also be the damage caused by the addition of AgNPs. It is hard to obtain higher spatial resolution with the present micro-sized SECM tip. A study of using a nanometre-sized SECM tip to analyse the local electrochemical reactivities is being undertaken in our laboratory.

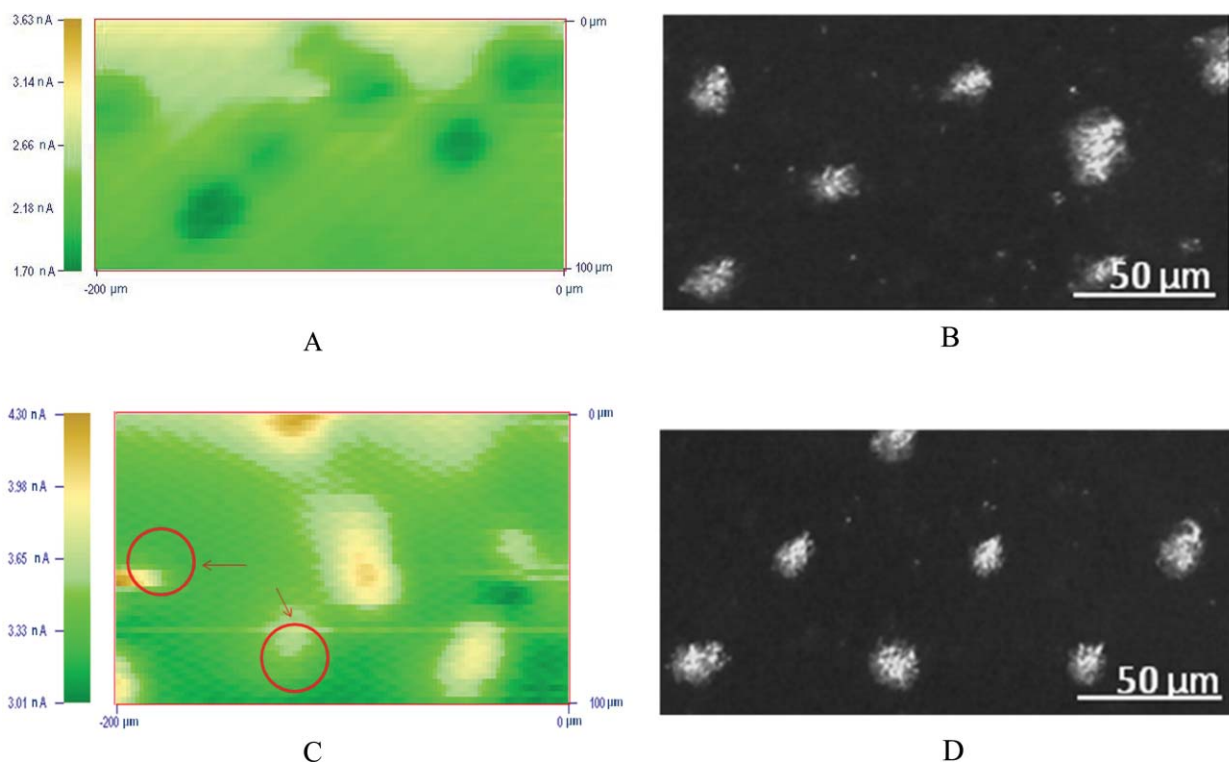


Fig. 6 Optical micrographs (B and D) and SECM images (A and C, 200 $\mu\text{m} \times 100 \mu\text{m}$) of island patterns of HeLa cells formed onto the Petri dish. The red circles in C indicate the lateral excursion of the cells after the interaction with AgNPs, which stands for the decreasing of the activities.

Conclusions

The interactions between HeLa cells and AgNPs have been investigated by SECM with the help of dual electro-active mediators as probing species. Fabrication of the cell array simplifies the study at single cell level and provides a platform for further investigations of interactions of AgNPs and other chemical substances, for instance, drugs. The variation of permeability of HeLa cell membranes after the interaction with AgNPs can be ignored because all the approach curves show little change under the concentration range of AgNPs studied in this work when $\text{Fe}(\text{CN})_6^{3-/4-}$ is used as the mediator; and the height of the cell is slightly decreased in this process. The approach curves are influenced by the AgNPs deposited on the HeLa cell, and the rate constants are increased with the increase of concentration of AgNPs in solution when K_3IrCl_6 is used as the mediator. This is due to IrCl_6^{2-} produced *in situ*, which can oxidize the AgNPs. A more detailed study about quantitative analysis of the interaction between AgNPs and the HeLa cells, and the interaction mechanism are being undertaken in our laboratory. Apparently, a much smaller size of SECM tip is necessary.

Acknowledgements

This work was supported by the National Natural Science Foundation of China (20735001, 20628506), the Foundation of Doctoral Programs of the Ministry of Education of China, and the special 985 project of Peking University.

References

- 1 B. R. Horrocks and G. Wittstock, Biological systems, in *Scanning Electrochemical Microscopy*, ed. A. J. Bard and M. V. Mirkin, Marcel Dekker, New York, 2001, p. 445.
- 2 S. Amemiya, J. Guo, H. Xiong and D. A. Gross, *Anal. Bioanal. Chem.*, 2006, **386**, 458.
- 3 A. J. Bard, X. Li and W. Zhan, *Biosens. Bioelectron.*, 2006, **22**, 461.
- 4 M. A. Edwards, S. Martin, A. L. Whitworth, J. V. Macpherson and P. R. Unwin, *Physiol. Meas.*, 2006, **27**, R63.
- 5 C. Lee, J. Kwak and A. J. Bard, *Proc. Natl. Acad. Sci. U. S. A.*, 1990, **87**, 1740.
- 6 H. Shiku, T. Shiraishi, H. Ohya, T. Matsue, H. Abe, H. Hoshid and M. Kobayashi, *Anal. Chem.*, 2001, **73**, 3751.
- 7 Y. Torisawa, T. Kaya, Y. Takii, D. Oyamatsu, M. Nishizawa and T. Matsue, *Anal. Chem.*, 2003, **75**, 2154.
- 8 T. Kaya, Y.-S. Torisawa, D. Oyamatsu, M. Nishizawa and T. Matsue, *Biosens. Bioelectron.*, 2003, **18**, 1379.
- 9 Y. Torisawa, H. Shiku, S. Kasai, M. Nishizawa and T. Matsue, *Int. J. Cancer*, 2004, **109**, 302.
- 10 H. Shiku, Y.-S. Torisawa, A. Takagi, S. Aoyagi, H. Abe, H. Hoshid, T. Yasukawa and T. Matsue, *Sens. Actuators, B*, 2005, **108**, 597.
- 11 H. Shiku, Y.-S. Torisawa, A. Takagi, S. Aoyagi, H. Abe, H. Hoshid, T. Yasukawa and T. Matsue, *Sens. Actuators, B*, 2005, **108**, 597.
- 12 T. Saito, C. Wu, H. Shiku, T. Yasukawa, M. Yokoo, T. Ito-Sasaki, H. Abe, H. Hoshid and T. Matsue, *Analyst*, 2006, **131**, 1006.
- 13 B. Liu, S. A. Rotenberg and M. V. Mirkin, *Proc. Natl. Acad. Sci. U. S. A.*, 2000, **97**, 9855.
- 14 B. Liu, S. A. Rotenberg and M. V. Mirkin, *Anal. Chem.*, 2002, **74**, 6340.
- 15 A. Pailleret, J. Oni, S. Reiter, S. Isik, M. Etienne, F. Bedioui and W. Schuhmann, *Electrochem. Commun.*, 2003, **5**, 847.
- 16 S. Isik, M. Etienne, J. Oni, A. Blöchl, S. Reiter and W. Schuhmann, *Anal. Chem.*, 2004, **76**, 6389.
- 17 S. Borgmann, I. Radtke, T. Erichsen, A. Blöchl, R. Heumann and W. Schuhmann, *ChemBioChem*, 2006, **7**, 662.

-
- 18 J. Mauzeroll and A. J. Bard, *Proc. Natl. Acad. Sci. U. S. A.*, 2004, **101**, 7862.
- 19 J. Mauzeroll, A. J. Bard, O. Owghadian and T. J. Monks, *Proc. Natl. Acad. Sci. U. S. A.*, 2004, **101**, 17582.
- 20 D. Zhan, X. Li, W. Zhan, F.-R. F. Fan and A. J. Bard, *Anal. Chem.*, 2007, **79**, 5225.
- 21 N. Gao, M. Zhao, X. Zhang and W. Jin, *Anal. Chem.*, 2006, **78**, 231.
- 22 X. Zhang, F. Sun, X. Peng and W. Jin, *Anal. Chem.*, 2007, **79**, 1256.
- 23 K. Nagamine, S. Onodera, A. Kurihara, T. Yasukawa, H. Shiku, R. Asano, I. Kumagai and T. Matsue, *Biotechnol. Bioeng.*, 2007, **96**, 1008.
- 24 K. Nagamine, N. Matsui, T. Kaya, T. Yasukawa, H. Shiku, T. Nakayama, T. Nishino and T. Matsue, *Biosens. Bioelectron.*, 2005, **21**, 145.
- 25 B. Liu, S. A. Rotenberg and M. V. Mirkin, *Anal. Chem.*, 2002, **74**, 6340.
- 26 J. Guo and S. Amemiya, *Anal. Chem.*, 2005, **77**, 2147.
- 27 M. Nishizawa, K. Takoh and T. Matsue, *Langmuir*, 2002, **18**, 3645.
- 28 P. Sun, F. O. Laforge, T. P. Abeyweera, S. A. Rotenberg, J. Carpino and M. V. Mirkin, *Proc. Natl. Acad. Sci. U. S. A.*, 2008, **105**, 443.
- 29 D. Falconnet, G. Csucs, H. M. Grandin and M. Textor, *Biomaterials*, 2006, **27**, 3044.
- 30 J. Hyun, H. Ma, Z. Zhang, T. P. Jr. Beebe and A. Chilkoti, *Adv. Mater.*, 2003, **15**, 576.
- 31 K. B. Holt and A. J. Bard, *Biochemistry*, 2005, **44**, 13214.
- 32 D. Ploton, M. Menager, P. Jeannesson, G. Himber, F. Pigeon and J. J. Adnet, *Histochem. J.*, 1986, **18**, 5.
- 33 A. Pich, L. Chiusa and E. Margaria, *Micron*, 2000, **31**, 133.
- 34 X.-H. N. Xu, W. J. Brownlow, S. V. Kyriacou, Q. Wan and J. J. Viola, *Biochemistry*, 2004, **43**, 10400.
- 35 J. R. Morones, J. L. Elechiguerra, A. Camacho, K. Holt, J. B. Kouri, J. T. Ramirez and M. J. Yacaman, *Nanotechnology*, 2005, **16**, 2346.
- 36 S. K. Gogoi, P. Gopinath, A. Paul, A. Ramesh, S. S. Ghosh and A. Chattopadhyay, *Langmuir*, 2006, **22**, 9322.
- 37 M. Zhang, G. Wittstock, Y. Shao and H. H. Girault, *Anal. Chem.*, 2007, **79**, 4833.
- 38 M. Zhang and H. H. Girault, *Electrochem. Commun.*, 2007, **9**, 1778.
- 39 H. Ma, J. Hyun, Z. Zhang, T. P. Jr. Beebe and A. Chilkoti, *Adv. Funct. Mater.*, 2005, **15**, 529.
- 40 J. Wang, F. Y. Song and F. M. Zhou, *Langmuir*, 2002, **18**, 6653.
- 41 J. F. Llopis and F. Colom, in *Encyclopedia of Electrochemistry of the Elements*, ed. A. J. Bard, Marcel Dekker, New York, 1976, vol. 6, p. 224.
- 42 J. M. Liebetrau, H. M. Miller, J. E. Baur, S. A. Takacs, V. Anupunpisit, P. A. Garris and D. O. Wipf, *Anal. Chem.*, 2003, **75**, 563.
- 43 R. T. Kurulugama, D. O. Wipf, S. A. Takacs, S. Pongmayteegul, P. A. Garris and J. E. Baur, *Anal. Chem.*, 2005, **77**, 1111.
- 44 L. P. Bauermann, W. Schuhmann and A. Schulte, *Phys. Chem. Chem. Phys.*, 2004, **6**, 4003.
- 45 A. Hengstenberg, C. Kranz and W. Schuhmann, *Chem.–Eur. J.*, 2000, **6**, 1547.